Correlation of Mechanical Factors and Gallbladder Pain

W G Li[a], X Y Luo*[b], N A Hill[b], A Smythe[c], S B Chin[a], A G Johnson[c] and N Bird[c]

[a] Department of Mechanical Engineering, University of Sheffield, Sheffield, S1 3JD, UK

[b] Department of Mathematics, University of Glasgow, Glasgow, G12 8QW, UK

[c] Academic Surgical Unit, Royal Hallamshire Hospital, Sheffield, S10 2JF, UK

*Corresponding Author:

Dr. X Y Luo
Department of Mathematics,
University of Glasgow,
Glasgow, G12 8QW, UK
Fax: +44 141 330 4111
E-mail: X.Y.Luo@maths.gla.ac.uk

Submitted on 28/06/2007

Abstract

Acalculous biliary pain occurs in patients with no gallstones, but is similar to that experienced by patients with gallstones. Surgical removal of the gallbladder (GB) in these patients is only successful in providing relief of symptoms to about half of those operated on, so a reliable pain-prediction model is needed. In this paper, a mechanical model is developed for the human biliary system during the emptying phase, based on a clinical test in which GB volume changes are measured in response to a standard stimulus and a recorded pain profile. The model can describe the bile emptying behaviour, the flow resistance in the biliary ducts, the peak total stress, including the passive and active stresses experienced by the gallbladder during emptying. This model is used to explore the potential link between gallbladder pain and mechanical factors. It is found that the peak total normal stress may be used as an effective pain indicator for gallbladder pain. When this model is applied to clinical data of volume changes due to CCK stimulation and pain from 37 patients, it shows a promising success rate of 88.2% in positive pain prediction.

Keywords: gallbladder, total stress, gallbladder pain, gallstone, flow resistance, emptying

1 Introduction

Human gallbladder pain is typically described as pain in the right upper part of the abdomen lasting for 30 minutes or more and provoked by a fatty meal, but not all patients experience these classical symptoms. Gallstones are the common cause, but only a small minority of the 10% of the population with stones experience pain. Gallbladder pain, also known as acalculous biliary or functional biliary pain, is defined as a steady pain located in the epigastrium and right upper quadrant in the absence of gallstones or when no other structural abnormalities exist in the biliary tract [1]. This pain may occur up to 7.6% in men and 20.7% in women, and has received great interest in recent years [2, 3]. Patients with gallbladder pain often pose diagnostic difficulties and undergo repeated ultrasound scans and oral cholecystograms. Sonography (oral cholecystography) combined with scintigraphy is commonly used to diagnose gallbladder pain. Reproduction of pain within 5-10 minutes of an injection of cholecystokinin (CCK) is also used to select a group of patients who may benefit from cholecystectomy [4].

However, surgery is often conducted without any guarantee of relieving the symptoms. Previous attempts to provide an accurate predictor for relief of gallbladder symptoms have not been successful with only about 50% of patients obtaining symptomatic relief following surgery [5]. Moreover some patients without stones appear to have typical gallbladder pain, but only half of them gain relief of their pain if the gallbladder is removed.
It is, therefore important to have a way of determining whether the pain is actually arising in the gallbladder, because similar symptoms can be produced by adjacent organs, such as the stomach. duodenum and pancreas, even without obvious disease.

Impaired motor function of gallbladder and sphincter of Oddi have long been suspected as a major factor contributing to gallbladder pain. The presumed mechanism for the pain is obstruction leading to distension and inflammation. The obstruction might result from a lack of co-ordination between the gallbladder and either the cystic duct or the sphincter of Oddi due to increased flow resistance or tone [2]. In other

words, pain may be produced by contraction against resistance or stretch of the gallbladder wall. When the gallbladder is inflamed, artificial distension produces gallbladder pain [6].

The pain provocation test has been used as a diagnostic tool to select patients with impaired gallbladder motor function who may benefit from the cholecystectomy. In the test CCK is injected intravenously to stimulate the gallbladder to contract and to induce the biliary pain. It is clinically accepted that when a gallbladder ejection fraction (percentage of the volume displaced during emptying) is less than 35% [7] or 40% [8], then the gallbladder motor function is considered to be impaired; otherwise, it is considered normal. It has been found that the gallbladder pain of some patients has been alleviated after their gallbladders are removed [7, 8]. However, conflicting reports also exist [3, 5, 9]. These facts suggest that impaired gallbladder motor function is not the only factor responsible for the pain.

As a type of visceral pain, gallbladder pain arises from the gallbladder and biliary tract with obstruction of the cystic or common bile ducts, which elevates pressure within the biliary system. Some researchers believe that the pain is directly related to intraluminal pressure of the biliary tract [10]. Gaensler (1951) examined the pain threshold of common bile duct for 40 patients before and after gallbladder removal. It was found that the pain threshold varied from 14.7 to 59 mmHg [11]. Csendes et al. (1979) illustrated that the pain threshold is in the range 15-60 mmHg [12]. The great variation in the pressure range in these studies suggests that the sensor of the pain in the biliary system may be better associated with other mechanical factors associated with the intraluminal pressure, but not directly to the pressure alone. Similar observations were made for pain in the oesophagus, duodenum, gastric antrum and rectum, which seems to respond to mechanoreceptors in the gastrointestinal tract wall [13]. These mechanoreceptors are found to depend on the luminal circumferential wall strain rather than pressure, tension and volume [13-17].

In this paper, we study gallbladder pain from the mechanical point of view, i.e. the human biliary system is considered as a pressure-flow dynamic system with a flexible wall. By estimating the peak total stress experienced by the muscle of the gallbladder, as well as other mechanical factors from a group of patients, we were able to identify

the mechanical factors most related to the pain felt by these patients. These estimates were based on the geometry changes during the emptying measured for different patients, and their correlations with the clinical observations of pain, which were provided by the Academic Surgical Unit of the Royal Hallamshire Hospital at Sheffield, UK.

2 Model and Method

2.1 Acquisition of clinical data during emptying

A CCK provocation test was carried on patients who had experienced repeated attacks of biliary-type pain in the absence of gallstones or any obvious causative findings [18]. After an overnight fast they were given an intravenous infusion of saline (control) followed by an intravenous infusion of CCK (0.05μg/kg body weight). Ultrasonography of the gallbladder was used to monitor changes in shape, initial volume, emptying and wall thickness at 15 minute intervals for 60 minutes. Note that pressure is not recorded in the experiments, which would require invasive techniques. The values of pressure for different subjects are predicted using the mechanical model (below) based on the volume and shape changes measured. The patients were unaware of which substance was being given and the test was only considered positive when the patients' usual 'gallbladder' pain was reproduced following CCK infusion.

Figure 1 illustrates schematically the pressure and volume variation with time during CCK provocation test. At point 1, the sphincter of Oddi is closed (see Fig. 2), the gallbladder is in a fasting state, and its volume, pressure and stresses all reach their minimum levels. Between 1 and 2, a small but positive pressure difference between the liver and the gallbladder exists, which allows the hepatic bile to be secreted slowly into the gallbladder. During this refilling, although the gallbladder volume is increasing, the pressure in gallbladder is more or less constant as the muscle relaxes. At the point 2, CCK is infused, which causes the gallbladder to contract. The pressure in the gallbladder rises rapidly up to point 3 in 3-5 minutes, and exceeds the pressure in the common bile duct. During this time, the sphincter of Oddi relaxes which lowers the pressure in the common bile duct further. The relative pressure in the gallbladder is now much higher than the common bile duct, and the emptying phase takes place. For most of the subjects, this lasts for about half an hour. The time scale for refilling is

usually the time lapse between two meals, and is often more than six times longer than emptying.

2.2 Mechanical Modelling

2.2.1 Predicting the pressure in gallbladder

Gallbladder emptying is caused by passive and active contractions due to the relaxation of stretch and CCK stimulation. The flow configuration in a biliary system is indicated in Fig. 2. During emptying, the bile flow rate out of the gallbladder, Q_{GB}, is equal to the flow rate into the duct, Q_{duct}, i.e.

$$-\frac{dV}{dt} = \frac{p - p_d}{R} \quad , \tag{1}$$

where R is the flow resistance, and p_d, the pressure in duodenum, is taken to be about 6mmHg [19]. Assuming that the gallbladder volume change rate, dV/dt, is related to the pressure drop rate dp/dt [20],

$$\frac{dV}{dt} = C\frac{dp}{dt} \quad , \tag{2}$$

where C is the constant compliance of the gallbladder, we have

$$C\frac{dp}{dt} + \frac{p - p_d}{R} = 0 \quad . \tag{3}$$

This is same as the *Windkessel* model for the cardio-vascular system [21]. The general solution of this linear ordinary differential equation is

$$p = p_d - \left(p_d - p_e\right)\exp((t_e - t)/RC) \, , \tag{4}$$

where p_e indicates the pressure when the gallbladder has completely emptied, which is chosen to be p_e=11mmHg [19], and t_e is the time taken for complete emptying. Complete emptying here means that the gallbladder volume V_e, at the end of emptying is $V_e = 0.3V_0$, where V_0 is the volume as the emptying begins. If a gallbladder is impaired, then the time taken for a complete emptying would be much longer than normal emptying time of about 30 minutes, i.e. its emptying will be incomplete when refilling starts.

In general, the gallbladder compliance, C, differs from one patient to another, but, as a first approximation, we take the average value measured by Middelfart et al. [22] for human gallbladder, C =2.731 ml/mmHg.

2.2.2 Gallbladder volume change and ejection fraction (EF)

From (2), (3), and (4), we can also solve for gallbladder volume,

$$V = C\left(p_e - p_d\right)\exp((t_e - t)/RC) + B \ , \tag{5}$$

where B is a constant, which is determined using the clinical measurements of gallbladder volume at $(0,V_0)$ and (t_e,V_e):

$$B = V_e - C\left(p_e - p_d\right) \ , \tag{6}$$

Substituting (6) into (5) we have

$$R = t/C \ln\left\{\frac{V_0 - B}{V - B}\right\}, \tag{7}$$

and

$$t_e = t \ln\left[\frac{V_0 - B}{C\left(p_e - p_d\right)}\right] / C \ln\left[\frac{V_0 - B}{V - B}\right] \ . \tag{8}$$

These measurements also allow us to calculated the gallbladder ejection fraction *EF* at 30 minutes after emptying as

$$EF = \frac{V_0 - V_{30}}{V_0} \times 100\% \ . \tag{9}$$

2.2.3 Estimating the passive peak stresses

In order to estimate the peak stresses in gallbladder muscle during emptying, we assume that the gallbladder is an ellipsoid with a thin uniform wall thickness, h_{GB}. The ellipsoid has a major axis D_1, and two minor axes, D_2 and D_3 ($D_1 \geq D_2 \geq D_3$). Using Cartesian coordinates as shown in Fig. 3, the mid-plane surface is described by

$$\begin{cases} x = 0.5D_1 \sin\theta\cos\varphi \\ y = 0.5D_2 \sin\theta\sin\varphi \\ z = 0.5D_3 \cos\theta \end{cases} \tag{10}$$

where θ and φ are the two independent angular variables for a point position on the surface, and θ is in the meridian plane and measured from the positive z axis,

$\theta \in [0, \pi]$; whereas φ is in the latitude plane, which is perpendicular to z axis, and measured from the first quadrant of $x-z$ plane, and $\varphi \in [0, 2\pi]$. The stresses in the ellipsoid surface under a uniform inner fluid pressure load p are given by [23],

$$\begin{cases} \sigma_\theta = \dfrac{pD_3 k_1 k_2}{4h_{GB}} \left[1 - \dfrac{k_1^2 - k_2^2}{k_1^2 k_2^2} \cos 2\varphi \right] F \\ \sigma_\varphi = \dfrac{pD_3}{4k_1 k_2 h_{GB}} \left[k_1^2 k_2^2 + \left(k_1^2 + k_2^2 - 2k_1^2 k_2^2 \right) \sin^2\theta + \left(k_1^2 - k_2^2 \right) \cos^2\theta \cos 2\varphi \right] \dfrac{1}{F} \\ \tau_{\theta\varphi} = \dfrac{pD_3}{4k_1 k_2 h_{GB}} \left(k_1^2 - k_2^2 \right) \cos\theta \sin 2\varphi \end{cases}, \tag{11}$$

where $k_1 = D_1/D_3$, $k_2 = D_2/D_3$ and F is

$$F = \frac{\sqrt{k_1^2 \cos^2\theta \cos^2\varphi + k_2^2 \cos^2\theta \sin^2\varphi + \sin^2\theta}}{\sqrt{k_1^2 \sin^2\varphi + k_2^2 \cos^2\varphi}} . \tag{12}$$

The mean wall thickness of healthy human gallbladder, h_{GB}, is taken to be 2.5mm [24]. The maximum normal stress is then

$$\sigma_{\max} = \max\left[\sigma_\theta, \sigma_\varphi \right] , \tag{13}$$

and the peak shear stress is

$$\tau_{\max} = \max[\tau_{\theta\varphi}] . \tag{14}$$

To estimate the values of $\sigma_{\max}$ and $\tau_{\max}$, the gallbladder domain was divided into 200×100 elements, and the values of the stresses were calculated from (11) at each node of the elements.

2.2.4 Contribution of the active normal stress

During emptying, the gallbladder contracts due to CCK, which induces the active stress. In this study, for simplicity, we will assume that all patients experience the same level of CCK stimulation, which induces the same peak active normal stress. Thus, we use a uniform response curve to CCK, estimated from experiments [25], as shown in Fig. 4. This curve can be interpolated using

$$\sigma_a = \begin{cases} \sigma_{a\max} \sin\left(\dfrac{\pi t}{2t_{CCK}} \right) & t \le t_{CCK} \\ \sigma_{a\max} \left(1 - \dfrac{t - t_{CCK}}{t_{dc}} \right) & t > t_{CCK} \end{cases} , \tag{15}$$

where $\sigma_{a\max}$ is the maximum active stress taken to be 8.82 mmHg, t_{CCK} and t_{dc} are chosen to be t_{CCK}=1min and t_{dc}=7.5min [26]. There are no reports on active shear stress due to CCK.

Finally, the total maximum normal stress in the gallbladder wall during the emptying is thus

$$\sigma_{t\max} = \sigma_{a\max} + \sigma_{\max} \ . \tag{16}$$

3 Results

The clinical data for 37 patients during emptying were provided by the Royal Hallamshire Hospital, Sheffield, UK. Based on these data, we have calculated various factors, summarized in Table 1.

All the initial gallbladder volumes are in the range of 15-35ml, except for those of subjects 19 and 35, which have an initial volume of 60ml and 10ml, respectively. The average initial gallbladder volume is 25.3ml. The gallbladder volume change versus time is plotted in Fig. 5, for three typical subjects: 1, 18 and 35, which indicates, respectively, poor, fair and super-emptying behaviour.

The flow resistance varies from 1.7 to 392.6 mmHg/ml/min, showing a significant variation across the subjects. The subjects with good emptying (large EF) have low flow resistance and those with poor emptying (small EF) usually present high resistance. In general the resistance is in the range of 20-70mmHg/ml/min. The average resistance is 53.4 mmHg/ml/min, however the resistances of subjects 1, 2, 3 and 5 are all higher than 130 mmHg. The resistance of the cystic duct of the prairie dog is found to increase from 50 to 120mmHg/ml/min when its gallbladder changed from healthy status to that with gallstones after feeding with a cholesterol diet [29]. Thus if we can extend the experimental finding for prairie dogs to human, then it is likely that these with higher resistances indicate the unhealthy states.

The maximum values of the pressure, $p_{\max}$, for all subjects are given in Table 1 and the pressure variation with time is illustrated in Fig. 6 for subjects 1, 18 and 35. It can be seen that the peak pressure of most of the gallbladders, except gallbladder 19, is in the range of 15-20mmHg. This agrees well with physiological values [19]. The gallbladder pressure of subjects 1-14, which have poor emptying, decrease more slowly with time. In general, the flatness of the pressure curves seems to be associated with poor emptying. In other words a gallbladder with poor-emptying is subject to a higher pressure for a longer period of time.

The gallbladder shapes in the subject group in Table 1 can be characterized by two main geometric types: those (type 1) for which $k_2 > 1$; and those (type 2) for which $k_2 \approx 1$. The peak normal stress level of first type is higher than that of second type, see Fig. 7 for subjects 28 (type 1) and 12 (type 2). The shear stress patterns for these two subjects are similar, with the maximum/minimum values occurring at the same place: $\theta = \varphi = 45^0$, but are very different from the normal stresses. This is because the maximum value of the normal stress is much more sensitive to the geometric changes, therefore its location and value can differ significantly for different geometric types.

When these factors are compared with the pain information from clinical observations in Table 1, it shows that the direct correlations with pain of the flow resistance, shear stress, and EF are all rather poor. The maximum pressure, $p_{\max}$, seems to be weakly correlated with pain. The most remarkable correlation, however, is found to be with the maximum normal stress $\sigma_{t\max}$.

In the following we consider three pain predications based on, 1) ejection fraction: *EF* < 35%, which is commonly used in clinics, 2) pressure: p >15.4mmHg (15.4mmHg is estimated when patients' average EF is 35%), and 3) maximum normal stress: $\sigma_{t\max} > \sigma^*$, where σ^* =200 mmHg is from an averaged value calculated from pressure measurement by Gaenseler [11]. The results of the predictions are listed in Tables 2-4.

From table 3, it is clear that all predictions using $\sigma_{t\max}$ are correct except for gall-bladders 12, 17, 18, 20, 22 and 35, thus out of 37 cases, 30 agree with the clinical observations. For comparison, if we use $EF < 35\%$ as the pain threshold, the results are far less positive, with less than half agreeing with clinical data. The correlations of the shear stress and resistance are also poor to pain. The results from using p> 15.4mmHg is better than using EF, but not as good as using $\sigma_{t\max}$.

In order to see how reliable these predictions are, below we analyse these from a more rigorous statistical standpoint, making use of the logistic transformation (see Appendix).

Table 5 is the 2×2 contingency table for the three pain related indices, EF, $p_{\max}$ and $\sigma_{t\max}$, where the counts of the success and failure based on clinical observations are listed. The corresponding success and failure rates are also listed in the bracket. It can be seen that the success rates of positive (pain) and negative (no-pain) predictions using EF is all less than 0.5. Therefore this index has no prediction power and should be rejected.

The success rates of the positive and negative predictions using $p_{\max}$ are somewhere between 0.5 and 0.7. Interestingly, the rate of its negative prediction is better than the positive prediction. However, for $\sigma_{t\max}$ both (positive and negative) the success rates are over 0.75, with the positive (pain) prediction as high as 0.882.

The 95% confidence intervals for the success rate of pain and no-pain predictions are shown in Table 6. The difference between the success rates of positive and negative predictions can be seen by using the ratio of odds from the two rows in the 2×2 contingency table (see Table 5). The inference for the odds ratio of positive (pain) and negative (no pain) predictions is summarized in Table 7 for both $p_{\max}$ and $\sigma_{t\max}$. The 95% confidence interval for odds ratio of success rate of positive (pain) and negative (no pain) prediction with $p_{\max}$ is (0.60, 0.769). i.e., using this index, the success rate of pain prediction is at least 23.1% less than no-pain prediction. Whilst with $\sigma_{t\max}$ this

is (1.373, 1.605), thus the success rate of pain prediction is 37.5% higher than no-pain prediction. This is important as in clinical diagnosis, the significance of a reliable positive prediction is much greater than the negative prediction. Therefore we believe that the peak normal stress is the better pain prediction compared with the maximum pressure.

4 Discussions

Our study shows that the peak normal stress is a good index to use for pain prediction. This prediction is correct for all but seven subjects (Table 4) in all 37 cases studied. A reason for the seven failed cases could be that these patients have slightly lower or higher pain threshold levels than the standard value used. It is also likely to be the simplifications introduced in the model, such as a uniform gallbladder compliance, and an elliptical gallbladder shape, which are used in the model for every subject, whereas in reality, should all be subject-dependent.

It is important to realise that the peak normal stresses in gallbladder wall not only depend on the pressure p, but also on its geometry, D_1, D_2 and D_3, and their relative ratios, see Table 1. In fact, we believe that it is through the normal stress mechanism that the effects from both the pressure and the geometry change come into play in producing pain. Additionally, it is interesting to note that a poor emptying rate (a lower ejection fraction) is not necessarily associated with the pain, subjects 1, 2, 3, 4, 7, 10, 11 and 12 have all showed poor emptying, but do not experience any pain, both from the model prediction, or from the clinical observation. The gallbladders with super emptying (a larger ejection fraction value) can also demonstrate pain, for instance, subjects 34 and 35. Therefore, the ejection fraction is not considered to be a good indicator for pain prediction. This is important since impaired gallbladder emptying is still used as the clinical criterion for cholecystectomy [1]. Our study clearly suggests that this criterion needs to be reviewed.

This is important, however, to point out that there are limitations in our current approach. We have assumed here that the gallbladder is an ellipsoid, which is a commonly adopted assumption in clinical practice (e.g. in real-time Ultrasonography). However, this approximation can cause an error up to 10% in estimates of gallbladder

size [32]. Our model can be improved if the gallbladder volume can be obtained more accurately, which may be possible with improved clinical instrumentation. In addition, although this model has included both active and passive stresses, the active stress is not obtained from the smooth muscle mechanics, rather it is taken to be a same typical form for all subjects applied uniformly over the gallbladder wall. In practice, this also varies with individual subject. There should be a range of values for the threshold stress at which patients can feel pain, i.e. the pain sensitivity is individual. Using a standard value of 200 mmHg here is only an approximation. If this value is allowed to change between 150-200mmHg, then the success rate of our prediction may be even higher (e.g. prediction for subject U may also be correct). Finally, the number of clinical samples that we have able to use over the last few years is still relatively small, being 37 only. For a more reliable pain prediction, more samples should be included. Further and more extensive studies from our and other groups are clearly required. Much greater knowledge about the smooth muscle function in the gallbladder, remodelling and growth during abnormal emptying, and the mechanical sensor related to the pain, as well as the individual pain threshold, are all required in order to understand the precise mechanism of the gallbladder pain.

Having mentioned all these limitations, it is encouraging that a simple model based on non-invasive clinical measurement (volume changes) may be used to predict the pain with 88.2% positive success rate for the samples studied.

5 Conclusions

In this paper, a simple gallbladder model is developed to evaluate the correlations of the mechanical factors with gallbladder pain, based on clinical data for 37 patients. These factors include the gallbladder pressure, ejection fraction, flow resistance, shear stress, and peak shear and normal stresses. It is found that the peak normal stress is the best mechanical factor that may be used to predict the gallbladder pain. Using this as a pain criterion, the agreement with 37 clinical observations (for positive prediction) is about 88.2%. On the other hand, it is found that, a poor emptying, the maximum pressure in gallbladder, the peak shear stress, and the flow resistance, do not correlate directly with pain. This is because the normal stress in gallbladder wall depends not only on the gallbladder pressure (i.e. flow resistance), but also on the gall-

bladder geometry. Although this is simple model and has only been tested for 37 patients, its simplicity, and the fact that it requires the minimum clinical data, makes it a promising potential as one of the routine clinical diagnostic methods.

Acknowledgement

We would like to thank SWANN MORTON Ltd and University of Glasgow for part of the financial support for this research. Helpful discussion with Dr. T. Aichison at the Department of Statistics, University of Glasgow is also greatly appreciated.

References

[1] Shaffer E, 2003, Acalculous biliary pain: new concepts for an old entity, ***Digestive and Liver Disease***, 35(Suppl 3), S20-S25.

[2] Corazzizri et al; Shaffer E A, Hogan W J, Sherman S and Toouli J, 1999, Functional disorders of the biliary tract and pancreas, ***Gut***, 45 (Suppl II), II48-II54.

[3] Rastogi A, Slivka A, Moser A J, Wald R, 2005, Controversies concerning pathophysiology and management of acalculous biliary-type abdominal pain, Digestive Diseases and Sciences, 50(8), 1391-1401.

[4] Williamson R C N, 1988, Acalculous disease of gall bladder, ***Gut***, 29, 860-872.

[5] Smythe A, Majeed A W, Fitzhenry M and Johnson A G, 1998, A requiem for the cholecystokinin provocation test ?, ***Gut***, 43, 571-574.

[6] Funch-Jensen P, 1995, Sphincter of Oddi physiology, Journal of Hepato-Biliary-Pancreatic ***Surgery***, 2, 249-254.

[7] Bingener J, Richards M L, Schwesinger W H and Sirinek K R, 2004, Laparoscopic cholecystectomy for biliary dyskinesia, ***Surgical Endoscopy***, 18, 802-806.

[8] Yap L, Wycherley A G, Morphett A D and Toouli J, 1991, Acalculous biliary pain: cholecystectomy alleviates symptoms in patients with abnormal cholescintigraphy, ***Gastroenterology***, 101, 786-793.

[9] Smythe Ahmed R, Fitzhenry M, Johnson A G and Majeed A W, 2004; Bethanechol provocation testing does not predict symptom relief after cholecystectomy for acalculous biliary pain, ***Digestive and Liver Disease***, 36, 682-686.

[10] Ness T J and Gebhart G F, 1990, Visceral Pain: a review of experimental studies, ***Pain***, 41, 167-234.

[11] Gaensler E A, 1951, Quantitative determination of the visceral pain threshold in man, ***Journal of Clinical Investigation***, 30, 406-420.

[12] Csendes A, Kruse A, Funch-Jensen P, Oster M J, Ornsholt J and Amdrup E, 1979, Pressure measurements in the biliary and pancreatic duct systems in controls and in patients with gallstones, previous cholecysterctomy, or common bile bile duct stones, ***Gastroenterology***, 77, 1203-1210.

[13] Drewes A M, Pedersen J, Liu W, Arendt-Nielsen L and Gregersen H, 2003, Controlled mechanical distension of human oesophagus: sensory and biomechanical findings, ***Scand Journal of Gastroenterology***, 38, 27-35.

[14] Barlow J D, Gregersen H and Thompson D G, 2001, Identification of the biomechanical factors associated with the perception of dstension in the human esophagus, ***American Journal Physiology***, 282, G683-G689.

[15] Petersen P, Gao C, Arendt-Nielsen L, Gregersen H and Drewes A M, 2003, Pain intensity and biomechanical response during ramp-controlled distension of the human rectum, ***Digestive Diseases and Sciences***, 48(7), 1310-1316.

[16] Gao C, Arendt-Nielsen L, Liu W, Petersen P, Drewes A M and Gregersen H, 2002, Sensory and biomechanical responses to ramp-controlled distension of the human duodenum, ***American Journal Physiology***, 284, G461-G471.

[17] Gregersen H, Hausken T, Yang J, Odegaard S and Giljia O H, 2006, Mechanosensory properties in the human gastric antrum evaluated using B-mode ultrasonography during volume-controlled antral distension, ***American Journal Physiology***, 290, G876-G882.

[18] Cozzolino H J, Goldstein F, Greening R R and Wirts C W, 1963, The cystic duct syndrome, ***JAMA***; 185, 920-924.

[19] Dodds W J, Hogan W J and Green J E, 1989, Motility of the biliary system: In: Handbook of Physiology: the gastrointestinal system; Schultz S G; Vol. 1, Section 6, Part 2(28); American Physiological Society, Betheda, Maryland, 1055-1101.

[20] Ryan J and Cohen S, 1976, Gallbladder pressure-volume response to gastrointestinal hormones, ***American Journal Physiology***, 230, 1461-1465.

[21] Fung Y C, 1984, Biodynamics Circulation, New York: Springer-Verlag, 22-23.

[22] Middelfart H V, Jensen P, Hojgaard L and Funch-Jensen P, 1998, Pain patterns after distension of the gallbladder in patients with acute cholecystis, ***Scand Journal of Gastroenterology***, 33, 982-987.

[23] Novozhilov V V, 1964, Thin Shell Theory, Groningen: P. Noordhoff LTD, 125-130.

[24] Deitch E A, 1981, Uitility and Accuracy of Ultrasonically Measured Gallbladder Wall as a Diagnostic Criteria in Biliary Tract Disease, ***Digestive Diseases and Sciences***, 26(8), 686-693.

[25] Matsumoto T, Sarna S K, Condon R E, Dodds W J and Mochinaga N, 1988, Canine gallbladder cyclic motor activity, ***American Journal Physiology***, 255, G409-G416.

[26] Milenov K and Shahbazian A, 1995, Cholinergic pathways in the effect of motilin on the canine ileum and gallbladder motility: in vivo and in vitro experiments, ***Comparative Biochemistry Physoioogy***, 112A(3/4), 403-410.

[27] Ferris D O and Vibert J C, 1959, The common bile duct: significance of its diameter, ***Annals of Surgery***, 149(2), 249-251.

[28] Mahour G H, Wakim K G and Ferris D O, 1967, The common bile duct in man: its diameter and circumference, ***Annals of Surgery***, 165(3), 415-419.

[29] Pitt H A, Doty J E, DenBesten L and Kuchenbecker S L, 1981, Stasis before gallstone formation: altered gallbladder compliance or cystic duct resistance, ***The American Journal of Surgery***, 143, 144-149.

[30] Inglfinger J A, Mosteller F, Thibodeau L A and Ware J H, 1987, Biostatistics in clinical medicine, New York: Macmillan Publishing Co. Inc., 140-148.

[31] Dawson-Saunders B and Trapp R G, 1994, Biostatistics, London: Prentice-Hall International Inc., 148-149.

[32] Everson G T, Braverman D Z, Johson M L and Kern F, 1980, A critical evaluation of real-time ultrsonography for the study of gallbladder volume and contraction, ***Gastroenterology***, 79, 40-46.

[33] Rohling R N, Gee A H and Berman L, 1998, Automatic registration of 3-D ultrasound images, ***Ultrasound in medicine & Biology***, 24(6), 841-854.

[34] Ichii H, Takada M, Kashiiwagi R, Sakane M, Tabata F, Ku Y, Fujimori T and Kuroda Y, 2002, Three-dimensional reconstruction of biliary tract using spiral computed tomography for laparoscopic cholecystectomy, ***World Journal of Surgery***, 26, 608-611.

[35] Liao D, Duch B U, SrodkildeJorgensen H, Zeng Y J, Gregersen H and Kassab G S, 2004, Tension and stress calculations in 3-D Fourier model of gallbladder geometry obtained from MR images, ***Annals of Biomedical Engineering,*** 32(5), 744-755.

Appendix: Logistic transformation [36][37]

From elementary statistics, we know that if we have a sample from a normal distribution with known variance σ^2, a 95% confidence interval for the mean μ is [37]

$$\bar{x} \pm 1.96 \frac{\sigma}{\sqrt{n}} \ . \tag{A1}$$

The quantity $\sigma/\sqrt{n}$ is called the standard error; it measures the variability of the sample mean $\bar{x}$ about the true mean μ. The number 1.96 comes from a table of the standard normal distribution; the area under the standard normal density curve between −1.96 and 1.96 is 95%.

The confidence interval (A1) is valid because over repeated samples the estimate $\bar{x}$ is normally distributed about the true value μ with a standard deviation of $\sigma/\sqrt{n}$.

When the sample size is small, we may be able to improve the quality of the approximation by applying a suitable reparameterization, a transformation of the parameter to a new scale. The "logistic" or "logit" transformation is such a transformation, defined as

$$\phi = \log\left(\frac{p}{1-p}\right) \ . \tag{A2}$$

Here $0 \le p \le 1$ and $-\infty < \phi < -\infty$. Solving (A2) for p produces the back-transformation,

$$p = \frac{e^{\phi}}{1+e^{\phi}} \ . \tag{A3}$$

Table A shows a 2×2 contingency table for the two variables A and B, with sample sizes n_1 (success) and n_2 (failure), and B with sample sizes n_3 (success) and n_4 (failure), respectively. We want to determine the endpoints of 95% confidence interval for success rates p_1 and p_2 as well as to compare them. The success rates are calculated from

$$p_1 = \frac{n_1}{n_1 + n_2} \ , \tag{A4}$$

and

Table A 2×2 contingency table for the variables A and B

Variable	Success	Failure	Sample size
A	$n_1 (p_1)$	$n_2 (1 - p_1)$	$n_1 + n_2$
B	$n_3 (p_2)$	$n_4 (1 - p_2)$	$n_3 + n_4$

$$p_2 = \frac{n_3}{n_3 + n_4} \ . \tag{A5}$$

The endpoints of the 95% confidence intervals for success rate p_1 are

$$p_{1low} = \frac{e^{p_1 - 1.96\sqrt{\frac{1}{p_1 (n_1 + n_2)(1 - p_1)}}}}{1 + e^{p_1 - 1.96\sqrt{\frac{1}{p_1 (n_1 + n_2)(1 - p_1)}}}} \ , \tag{A6}$$

and

$$p_{1high} = \frac{e^{p_1 + 1.96\sqrt{\frac{1}{p_1 (n_1 + n_2)(1 - p_1)}}}}{1 + e^{p_1 + 1.96\sqrt{\frac{1}{p_1 (n_1 + n_2)(1 - p_1)}}}} \ . \tag{A7}$$

The endpoints of 95% confidence interval for success rate p_2 (variable B) are

$$p_{2low} = \frac{e^{p_2 - 1.96\sqrt{\frac{1}{p_2 (n_3 + n_4)(1 - p_2)}}}}{1 + e^{p_2 - 1.96\sqrt{\frac{1}{p_2 (n_3 + n_4)(1 - p_2)}}}} \ , \tag{A8}$$

and

$$p_{2high} = \frac{e^{p_2 + 1.96\sqrt{\frac{1}{p_2 (n_3 + n_4)(1 - p_2)}}}}{1 + e^{p_2 + 1.96\sqrt{\frac{1}{p_2 (n_3 + n_4)(1 - p_2)}}}} \ . \tag{A9}$$

The difference between success rate of A and B can be distinguished by using the ratio of odds from the two rows in Table 1. The asymptotic standard error of two samples is [36]

$$\sigma = \log\left(\sqrt{\frac{1}{n_1}+\frac{1}{n_2}+\frac{1}{n_3}+\frac{1}{n_4}}\right), \tag{A10}$$

and the ratio of odds from two samples is [36]

$$\theta = \log\left[\frac{p_1(1-p_2)}{(1-p_1)p_2}\right]. \tag{A11}$$

The endpoints of 95% confidence interval for the ratio of odds are [36]

$$\theta_{low} = e^{\theta-1.96\sigma}, \tag{A12}$$

and

$$\theta_{high} = e^{\theta+1.96\sigma}. \tag{A13}$$

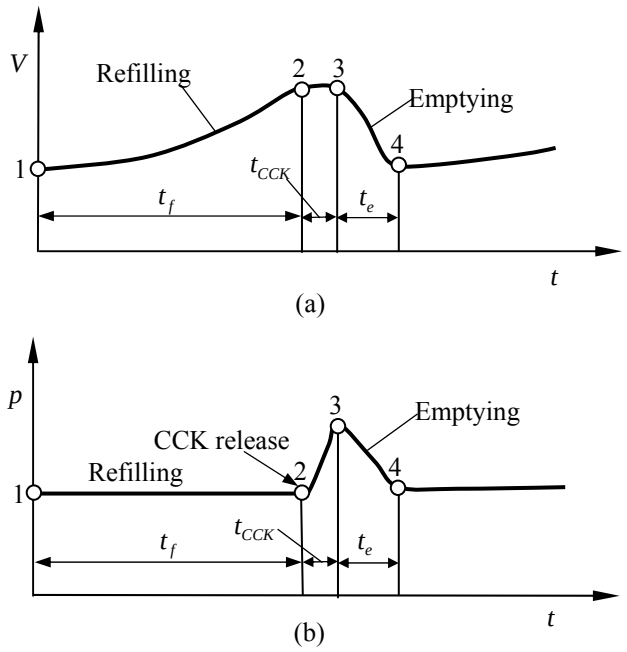

Fig. 1 Diagrammatic representation of gallbladder refilling and emptying. Refilling starts at point 1 and stops at point 2. Emptying begins at point 2 and lasts until point 4, when the next refilling starts. Note t_f is the refilling time, and t_e is the emptying time, $t_f \approx 6t_e$.

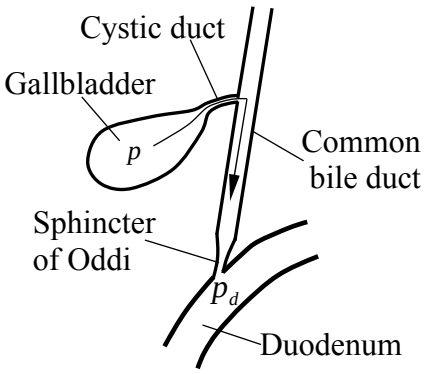

Fig. 2 Bile flows into the duodenum from the gallbladder through the cystic and common bile ducts due to the pressure difference $p - p_d$.

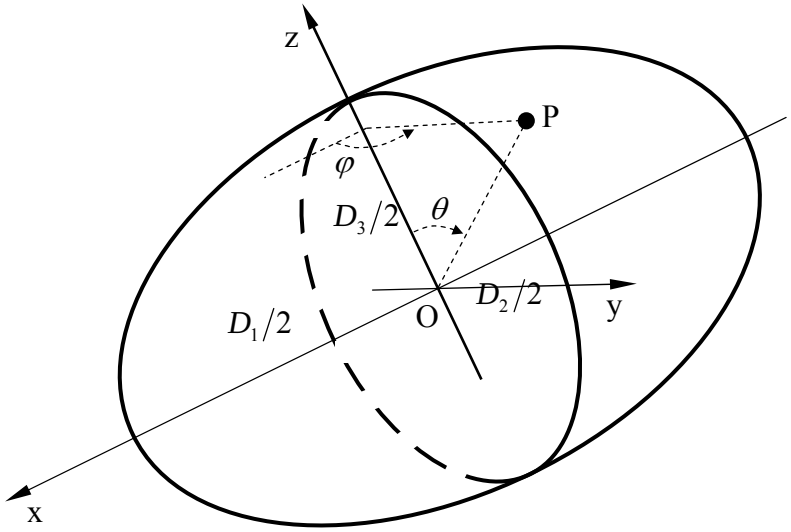

Fig. 3 Gallbladder shape is assumed to be ellipsoidal during emptying, the major axis length is D_1, the minor axes length are D_2, and D_3 ($D_1 > D_2 \geq D_3$), the gallbladder is subjected to a uniform internal pressure. The stress due to this pressure at a point P has three components: σ_θ (meridian), σ_φ (latitude), and $\tau_{\theta\varphi}$ (in surface).

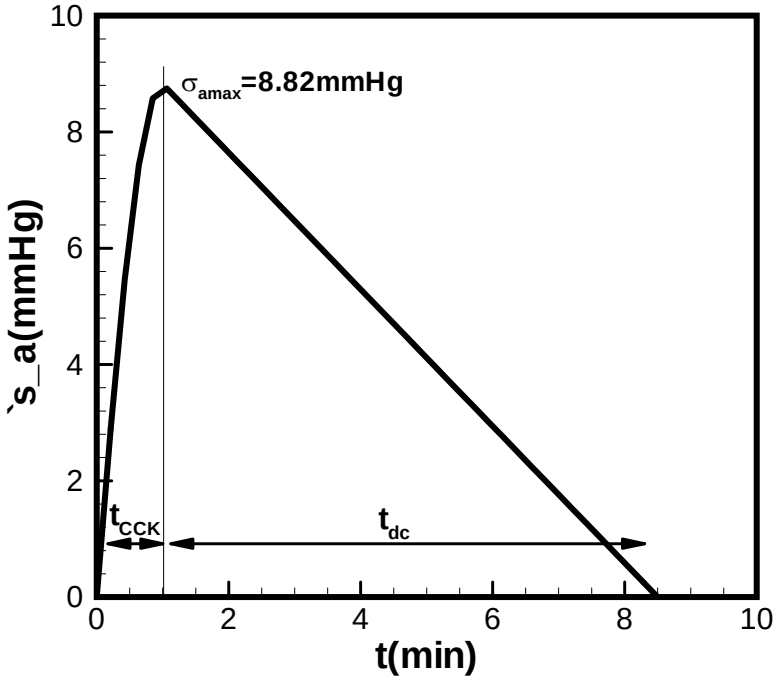

Fig. 4 Gallbladder response curve to CCK [26]. t_{CCK} is the CCK response time, and t_{dc} is the CCK decaying time, and $\sigma_{a\max}$ the peak active stress.

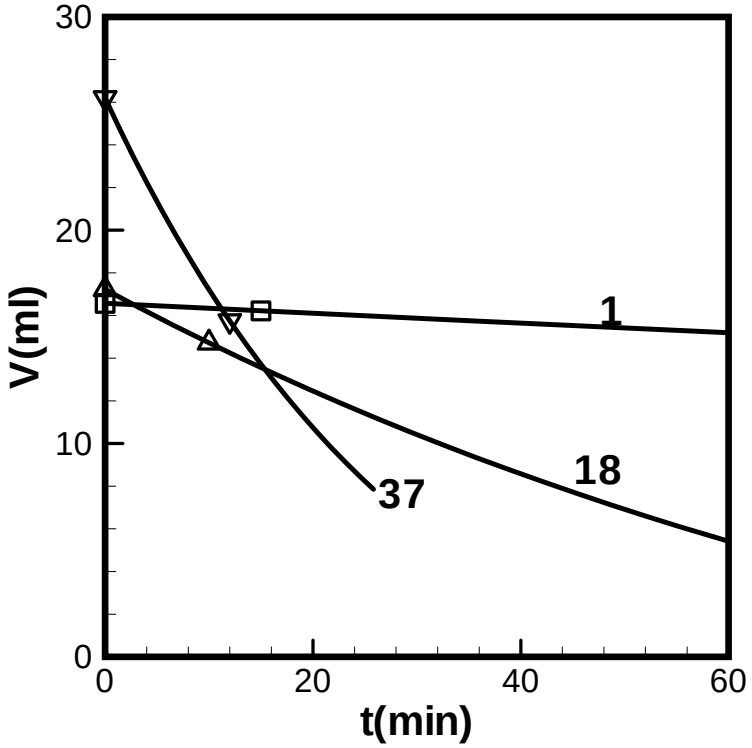

Fig. 5 Gallbladder volume variation with time during emptying for 3 typical subjects. The symbols are the experimental data and the solid curves are from (5).

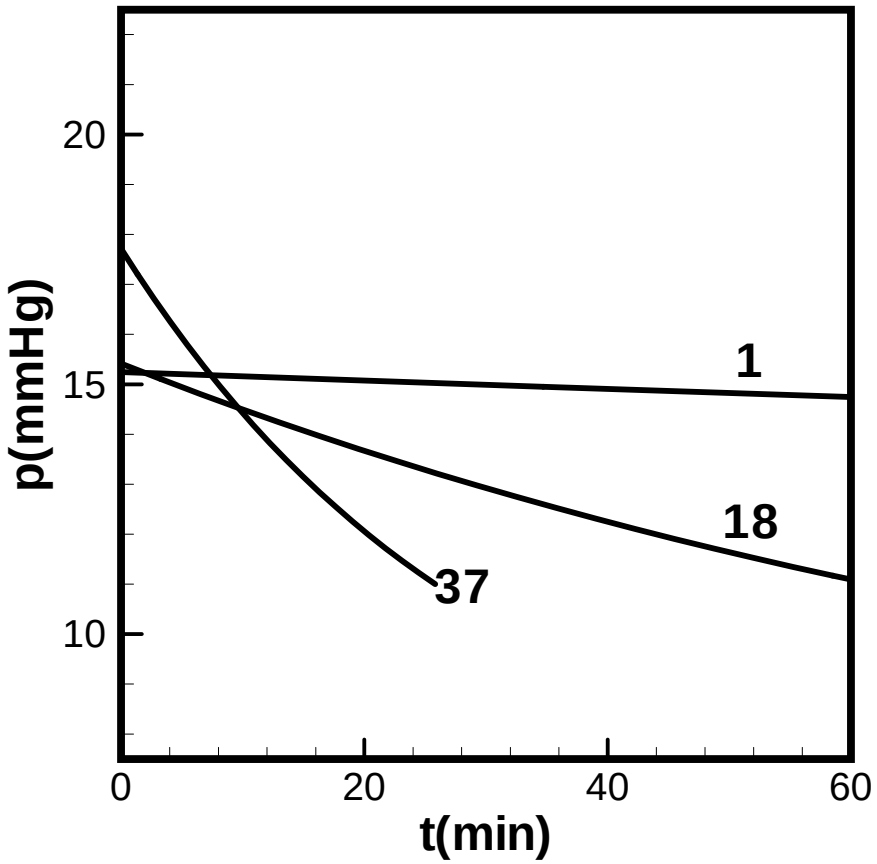

Fig. 6 The pressure variation with time emptying for subjects 1, 18, and 37, respectively.

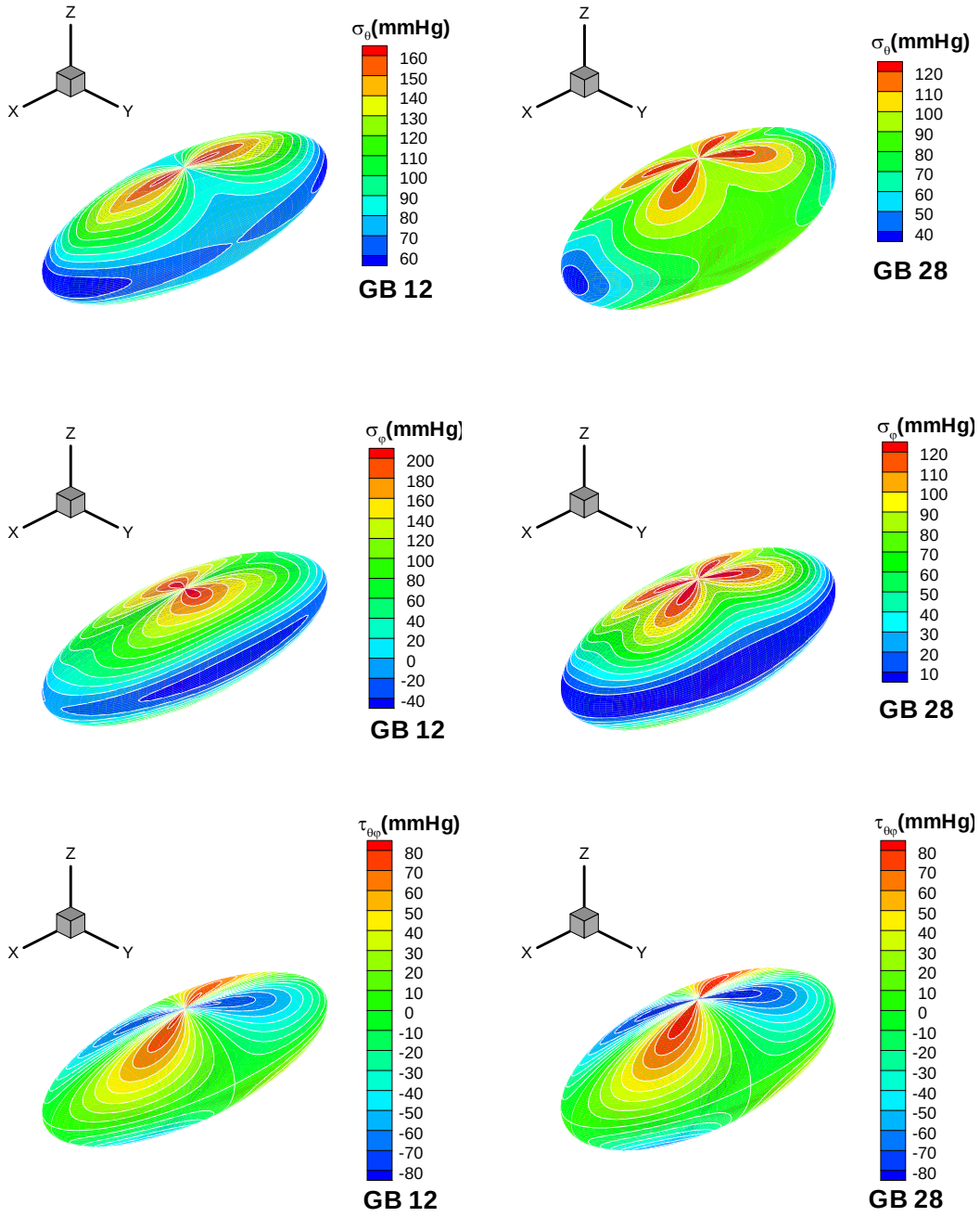

Fig. 7 The stresses contours on the gallbladder wall at the strat of emptying for subjects 12 (left) and 28 (right). The top frame is the principal stress σ_θ, the middle frame is the principal stress, σ_φ, and the bottom one is the shear stress $\tau_{\theta\varphi}$.

Table 1 Major parameters of gallbladder during the emptying

GB	V_0 (ml)	t (min)	EF (%)	R	D_1 (mm), k_1, k_2	$p_{\max}$ (mmHg)	$\sigma_{t\max}$ (mmHg)	$\tau_{\max}$ (mmHg)	Clinical observation
1	16.6	15	4.2	392.6	54.1,2.31,1.07	15.2	92.9	52.9	No pain
2	33.0	20	5.5	217.6	59.7,2.01,1.19	19.4	142.7	54.7	No pain
3	25.5	22	9.7	134.1	72.2,2.81,1.02	17.5	130.7	94.4	No pain
4	36.8	27	12.2	90.7	64.9,2.01,1.04	20.4	141.6	81.8	No pain

Table 2 Gallbladder pain prediction by using bile ejection fraction (EF)

GB	*EF* (%)	Pain prediction	Clinical observation	Agreement
1	4.2	Positive	Negative	No
2	5.5	Positive	Negative	No
3	9.7	Positive	Negative	No
4	12.2	Positive	Negative	No

Table 3 Gallbladder pain prediction by using the peak pressure

GB	$p_{\max}$ (mmHg)	Pain predicted	Clinical observation	Agreement
35	13.6	Negative	Positive	No
16	14.2	Negative	Negative	Yes
5	14.4	Negative	Positive	No
21	15.0	Negative	Negative	Yes
1	15.2	Negative	Negative	Yes
10	15.3	Negative	Negative	Yes
18	15.4	Positive	Positive	Yes
32	15.7	Positive	Negative	No
34	15.9	Positive	Positive	Yes
13	16.2	Positive	Positive	Yes
6	16.4	Positive	Positive	Yes
14	16.5	Positive	Positive	Yes
31	16.5	Positive	Positive	Yes
12	16.6	Positive	Negative	No
17	16.6	Positive	Positive	Yes
27	16.9	Positive	Positive	Yes
9	17.1	Positive	Positive	Yes
36	17.1	Positive	Negative	No
20	17.2	Positive	Positive	Yes
29	17.2	Positive	Negative	No
3	17.5	Positive	Negative	No
33	17.6	Positive	Negative	No
28	17.7	Positive	Negative	No
37	17.7	Positive	Negative	No
30	17.8	Positive	Positive	Yes
24	18.3	Positive	Negative	No
15	18.4	Positive	Positive	Yes
26	18.7	Positive	Positive	Yes
7	18.9	Positive	Negative	No
2	19.4	Positive	Negative	No
22	19.5	Positive	Positive	Yes
8	19.6	Positive	Positive	Yes
23	19.7	Positive	Positive	Yes
11	20.3	Positive	Negative	No
4	20.4	Positive	Negative	No
25	22.0	Positive	Positive	Yes
19	26.3	Positive	Positive	Yes

Table 4 Pain predictions by using the peak normal stress

GB	$\sigma_{t\max}$ (mmHg)	Pain predicted	Clinical observation	Agreement
21	82.9	Negative	Negative	Yes
16	85.7	Negative	Negative	Yes
1	92.9	Negative	Negative	Yes

Table 5 Counts, success rate of positive (pain) and negative (no-pain) prediction by using the five indices

Variable	Prediction	Success	Failure	Sample size
EF	Positive (pain)	7(0.438)	9(0.562)	16
	Negative (no pain)	8(0.381)	13(0.619	21
$p_{\max}$	Positive (pain)	18(0.581)	13(0.219)	31
	Negative (no pain)	4(0.667)	2(0.333)	6
$\sigma_{t\max}$	Positive (pain)	15(0.882)	2(0.118)	17
	Negative (no pain)	15(0.75)	5(0.25)	20

Table 6 95% confidence intervals of the success rate of positive (pain) and negative (no-pain) prediction

Variable	Success rate of positive(pain) and negative(no-pain) prediction	Confidence interval
EF	0.438	(0.225, 0.677)
	0.381	(0.203, 0.598)
$p_{\max}$	0.581	(0.405, 0.739)
	0.667	(0.268, 0.916)
$\sigma_{t\max}$	0.882	(0.631, 0.970)
	0.75	(0.522, 0.892)

Table 7 Inference for the odds ratio of positive (pain) and negative(no pain) prediction

Variable	Odds ratio of sample	Asymptotic standard error of sample	95% confidence interval for odds ratio with normal distribution
$p_{\max}$	-0.386	-0.063	(0.60, 0.769)
$\sigma_{t\max}$	0.396	-0.0395	(1.375, 1.605)